

Graphical Abstract

Attitude Control of a 3-DoF Quadrotor Platform using a Linear Quadratic Integral Differential Game Approach

Ali BaniAsad, Alireza Sharifi, Reza Pordal, Hadi Nobahari

Attitude Control of a 3-DoF Quadrotor Platform using a Linear Quadratic Integral Differential Game Approach

Ali BaniAsad, Alireza Sharifi, Reza Pordal, Hadi Nobahari

^aDepartment of Aerospace Engineering Sharif University of Technology, Tehran, Iran

Abstract

In this study, a linear quadratic integral differential game approach is applied to regulate and track the attitude angle of an experimental platform of the quadrotor using two players. One produces commands for each channel of the quadrotor and another creates the worst disturbance by minimizing a quadratic criterion with integral action. For this purpose, first, the attitude dynamics of the platform are modeled and its parameter is identified based on the Nonlinear Least Squares Trust-Region Reflective method. The performance of the proposed controller is evaluated for regulation and tracking problems. The ability of the controller is examined in the disturbance rejection. Moreover, the influence of uncertainty modeling is studied on the obtained results. Then, the performance of the proposed controller is compared with the classic PID, Linear Quadratic Regulator, and Linear Quadratic Integral Regulator. The result demonstrates the effectiveness of the Game Theory on the Linear Quadratic Regulator approach when the input disturbance occurs.

Keywords:

Linear Quadratic controller, Differential Game Theory, Quadrotor, three-degree-of-freedom Experimental Platform, Attitude Control.

1. Introduction

In this paper, an LQIR method, called LQIR-DG controller is suggested to produce the optimal and robust control command, i.e. rotational velocity command using the game theory approach. Since the LQIR-DG controller is affected by an exact model of the plant, the quadrotor's experimental platform is modeled and its parameters are identified based on experimental data. For control purposes, its linear state-space form is extracted using linearization of the nonlinear UAV model. Then, the LQIR-DG technique is applied in real-time to the experimental platform. The performance of the LQIR-DG method is evaluated in the presence of the disturbance and modeling error for regulation and tracking purposes. A comparison is also performed between the results of the classical PID, LQR, and LQIR and the proposed approach in real-time mode. The results show the proposed control structure is effective in the control of the quadrotor platform.

This research is organized as follows: section 2 presents the problem statement. In section 3, the dynamic platform is modeled. Then, the presented controller architecture is denoted in section 4. In sections 5 and 6, numerical results and a conclusion are represented, respectively.

2. Problem Statement

The experimental quadrotor platform rotates freely with rotational velocity about its roll, pitch, and yaw axes, according to Figure 1. The angular velocities in the body frame (p, q, r) and the euler angles (ϕ, θ, ψ)

Email addresses: ali.baniasad@ae.sharif.edu (Ali BaniAsad), ar.sharifi@sharif.edu (Alireza Sharifi), email address (Reza Pordal), nobahari@sharif.edu (Hadi Nobahari)

are measured using an Attitude Heading Reference System (AHRS). The measured states are utilized in the structure of the proposed controller to stabilize the quadrotor platform. The graphical abstract of the LQIR-DG controller structure is depicted in Figure 2.



Figure 1: 3DoF Quadrotor platform.

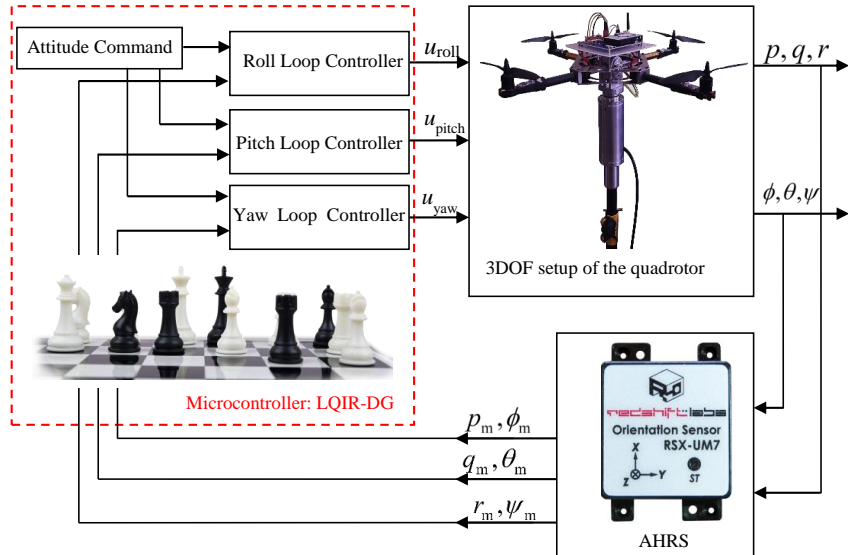


Figure 2: Graphical Abstract of the LQIR-DG Controller

3. Model of the Quadrotor Platform

Here, the quadrotor platform is modelled as nonlinear. Then, a state-space model and a linear model are developed for control purposes to be utilized in the controller strategy. Finally, a nonlinear identification method is applied to identify the parameters of the quadrotor.

3.1. Quadrotor configuration

According to Figure 3, the 3DoF quadrotor schematic is including four rotors rotating the z_B axis in the body frame with a rotational velocity, Ω . To eliminate the yawing moment, rotors (2, 4) and (1, 3) rotate clockwise and counter clockwise, respectively.

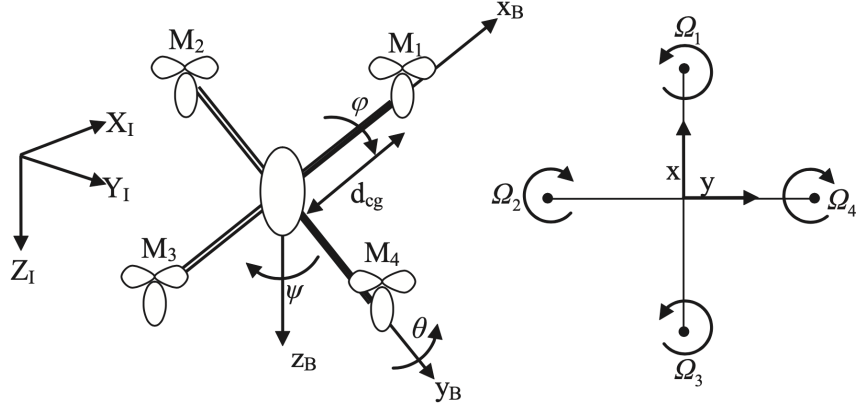


Figure 3: Quadrotor Configuration.

3.2. Dynamic Modeling of the Quadrotor Platform

Here, according to Newton-Euler, the model of the quadrotor platform is presented as follows [2, 1]:

$$\dot{p} = \frac{I_{yy} - I_{zz}}{I_{xx}} qr + q \frac{I_{\text{rotor}}}{I_{xx}} \Omega_{c,r} + \frac{b d_{cg} (\Omega_{c,2}^2 - \Omega_{c,4}^2)}{I_{xx}} + \frac{d_{\text{roll}}}{I_{xx}} \quad (1)$$

$$\dot{q} = \frac{I_{zz} - I_{xx}}{I_{yy}} rp + p \frac{I_{\text{rotor}}}{I_{xx}} \Omega_{c,r} + \frac{b d_{cg} (\Omega_{c,1}^2 - \Omega_{c,3}^2)}{I_{yy}} + \frac{d_{\text{pitch}}}{I_{yy}} \quad (2)$$

$$\dot{r} = \frac{I_{xx} - I_{yy}}{I_{zz}} pq + \frac{d (\Omega_{c,1}^2 - \Omega_{c,2}^2 + \Omega_{c,3}^2 - \Omega_{c,4}^2)}{I_{zz}} + \frac{d_{\text{yaw}}}{I_{zz}} \quad (3)$$

where $\Omega_{c,i}$ ($i = 1, 2, 3, 4$) is the rotational velocity, computed as

$$\Omega_{c,1}^2 = \Omega_{\text{mean}}^2 + \frac{1}{2b d_{cg}} u_{\text{pitch}} + \frac{1}{4d} u_{\text{yaw}} \quad (4)$$

$$\Omega_{c,2}^2 = \Omega_{\text{mean}}^2 + \frac{1}{2b d_{cg}} u_{\text{roll}} - \frac{1}{4d} u_{\text{yaw}} \quad (5)$$

$$\Omega_{c,3}^2 = \Omega_{\text{mean}}^2 - \frac{1}{2b d_{cg}} u_{\text{pitch}} + \frac{1}{4d} u_{\text{yaw}} \quad (6)$$

$$\Omega_{c,4}^2 = \Omega_{\text{mean}}^2 - \frac{1}{2b d_{cg}} u_{\text{roll}} - \frac{1}{4d} u_{\text{yaw}} \quad (7)$$

In the above equation, Ω_{mean} is rotational velocity of the rotors. Also, d_{cg} , d , and b represent the distance between the rotors and the gravity center, drag factor, and thrust factor, respectively. d_{roll} , d_{pitch} , and d_{yaw} denote the disturbances produced in the body coordinate frame. Additionally, u_{roll} , u_{pitch} , and u_{yaw} are control commands generated by the LQIR-DG controller. I_{rotor} is rotor inertia, and I_{xx} , I_{yy} , and I_{zz} are the moments of inertia. Euler angle rates are also determined from angular body rates as follows:

$$\begin{bmatrix} \dot{\phi} \\ \dot{\theta} \\ \dot{\psi} \end{bmatrix} = \begin{bmatrix} 1 & \sin(\phi) \tan(\theta) & \cos(\phi) \tan(\theta) \\ 0 & \cos(\phi) & -\sin(\phi) \\ 0 & \sin(\phi)/\cos(\theta) & \cos(\phi)/\cos(\theta) \end{bmatrix} \begin{bmatrix} p \\ q \\ r \end{bmatrix} \quad (8)$$

The residual rotor velocity, denoted by $\Omega_{c,r}$, is calculated as follows:

$$\Omega_{c,r} = -\Omega_{c,1} + \Omega_{c,2} - \Omega_{c,3} + \Omega_{c,4} \quad (9)$$

3.3. State-Space Formulation

By defining $\mathbf{x}_{\text{roll}} = [x_1 \ x_2]^T = [p \ \phi]^T$, $\mathbf{x}_{\text{pitch}} = [x_3 \ x_4]^T = [q \ \theta]^T$, and $\mathbf{x}_{\text{yaw}} = [x_5 \ x_6]^T = [r \ \psi]^T$, the formulation of the quadrotor platform is presented as follows:

$$\dot{x}_1 = \Gamma_1 x_3 x_5 + \Gamma_2 x_3 \Omega_r + \Gamma_3 b d_{\text{cg}} (\Omega_{c,1}^2 - \Omega_{c,3}^2) + \Gamma_3 d_{\text{roll}} \quad (10)$$

$$\dot{x}_2 = x_1 + (x_3 \sin(x_2) + x_3 \cos(x_2)) \tan(x_4) \quad (11)$$

$$\dot{x}_3 = \Gamma_4 x_1 x_5 - \Gamma_5 x_1 \Omega_r + \Gamma_6 b d_{\text{cg}} (\Omega_{c,2}^2 - \Omega_{c,4}^2) + \Gamma_6 d_{\text{pitch}} \quad (12)$$

$$\dot{x}_4 = x_3 \cos(x_4) - x_5 \sin(x_2) \quad (13)$$

$$\dot{x}_5 = \Gamma_7 x_1 x_3 + \Gamma_8 d (\Omega_{c,1}^2 - \Omega_{c,2}^2 + \Omega_{c,3}^2 - \Omega_{c,4}^2) + \Gamma_8 d_{\text{yaw}} \quad (14)$$

$$\dot{x}_6 = (x_3 \sin(x_4) + x_5 \cos(x_2)) / \cos(x_4) \quad (15)$$

where $\Gamma_i (i = 1, \dots, 8)$ is defined as:

$$\begin{aligned} \Gamma_1 &= \frac{I_{yy} - I_{zz}}{I_{xx}}, & \Gamma_2 &= \frac{I_{\text{rotor}}}{I_{xx}}, & \Gamma_3 &= \frac{1}{I_{xx}} \\ \Gamma_4 &= \frac{I_{zz} - I_{xx}}{I_{yy}}, & \Gamma_5 &= \frac{I_{\text{rotor}}}{I_{xx}}, & \Gamma_6 &= \frac{1}{I_{yy}} \\ \Gamma_7 &= \frac{I_{xx} - I_{yy}}{I_{zz}}, & \Gamma_8 &= \frac{1}{I_{zz}} \end{aligned} \quad (16)$$

The measurement vector, obtained from the AHRS, is presented as follows:

$$\mathbf{z} = [p \ q \ r \ \phi \ \theta \ \psi]^T + \boldsymbol{\nu} \quad (17)$$

where $\boldsymbol{\nu}$ is a Gaussian white noise. Moreover, the superscripts T indicate the transpose notation.

3.4. Linear Model

By defining $\dot{\mathbf{x}} = [\dot{\mathbf{x}}_{\text{roll}} \ \dot{\mathbf{x}}_{\text{pitch}} \ \dot{\mathbf{x}}_{\text{yaw}}]^T$, the linear model of the quadrotor platform represented about the equilibrium points ($\mathbf{x}_e^* = 0$ and $\mathbf{u}_e^* = 0$) as

$$\dot{\mathbf{x}} = \mathbf{A} \mathbf{x} + \mathbf{B} (\mathbf{u} + \mathbf{d}) \quad (18)$$

\mathbf{A} is the dynamic system matrix, denoted as

$$\mathbf{A} = \begin{bmatrix} \mathbf{A}_{\text{roll}} & \mathbf{0} & \mathbf{0} \\ \mathbf{0} & \mathbf{A}_{\text{pitch}} & \mathbf{0} \\ \mathbf{0} & \mathbf{0} & \mathbf{A}_{\text{yaw}} \end{bmatrix} \quad (19)$$

$\mathbf{A}_{\text{roll}} = \mathbf{A}_{\text{pitch}} = \mathbf{A}_{\text{yaw}} = \begin{bmatrix} 0 & 0 \\ 1 & 0 \end{bmatrix}$. Also, \mathbf{B} is the input matrix defined as

$$\mathbf{B} = \begin{bmatrix} \mathbf{B}_{\text{roll}} & \mathbf{0} & \mathbf{0} \\ \mathbf{0} & \mathbf{B}_{\text{pitch}} & \mathbf{0} \\ \mathbf{0} & \mathbf{0} & \mathbf{B}_{\text{yaw}} \end{bmatrix} \quad (20)$$

where $\mathbf{B}_{\text{roll}} = \begin{bmatrix} 1 & 0 \\ I_{xx} & 0 \end{bmatrix}^T$, $\mathbf{B}_{\text{pitch}} = \begin{bmatrix} 1 & 0 \\ I_{yy} & 0 \end{bmatrix}^T$, and $\mathbf{B}_{\text{yaw}} = \begin{bmatrix} 1 & 0 \\ I_{zz} & 0 \end{bmatrix}^T$.

3.5. Identification of the Platform Parameters

In this section, the Nonlinear Least Squares (NLS) algorithm is utilized for estimating the model parameters (Γ) of the 3DoF experimental platform using experimental data. This technique is based on the Trust-Region Reflective (TRR) method, which finds the best values for

$$\Gamma$$

by minimizing a cost function, defined as:

$$\min_{\Gamma_i} (\| e(\Gamma_i) \|^2) = \min_{\Gamma_i} \left(\sum_{j=1}^n (\mathbf{z}_j - \hat{\mathbf{z}}_j)(\mathbf{z}_j - \hat{\mathbf{z}}_j)^T \right) \quad (21)$$

where \mathbf{z} and $\hat{\mathbf{z}}$ are the experimental and simulated output signals, when the same input signals are applied ones. Moreover, j is the number of scenarios. To find a vector Γ , the optimization process performs until convergence is achieved. The structure of the identification approach is illustrated in figure 4

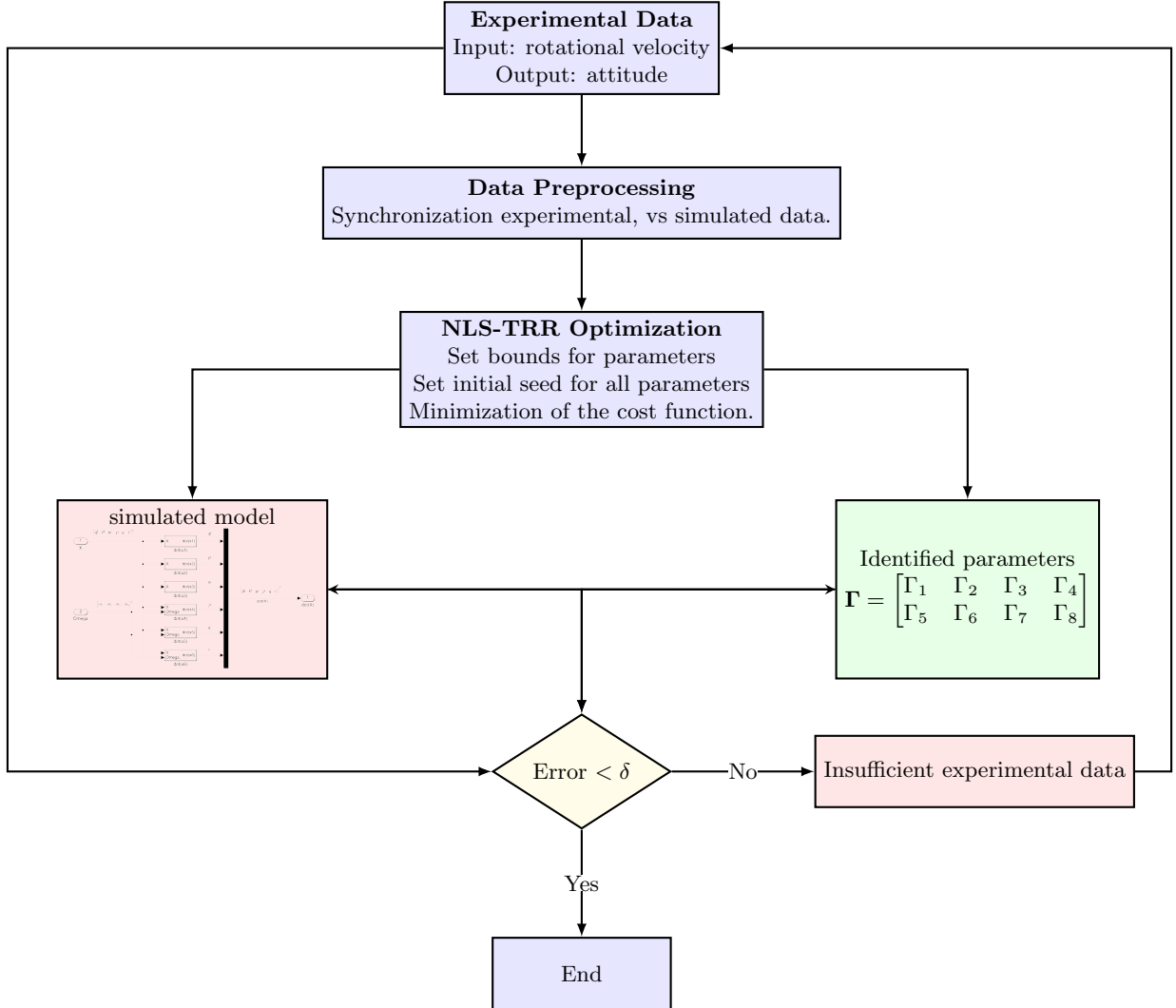


Figure 4: Structure of TRRLS identification approach.

4. LQIR-DG Controller Structure

First, the augmented states of the quadrotor platform, including the states and their integrals are selected to use in the structure of the LQIR-DG controller for eliminating the steady states errors. Then, the design methodology of the controller structure is introduced to produce the optimal commands for the 3DoF quadrotor platform.

4.1. Augmented States

To augment an integral action into the control strategy architecture, the augmented states are defined as $\mathbf{x}_a = \begin{bmatrix} \mathbf{x} & \int \mathbf{x} \end{bmatrix}^T$. Then, the model of the quadrotor platform, utilized in the controller structure, is presented as

$$\dot{\mathbf{x}}_a = \begin{bmatrix} \mathbf{A} & \mathbf{0} \\ \mathbf{I} & \mathbf{0} \end{bmatrix} \mathbf{x}_a + \begin{bmatrix} \mathbf{B} \\ \mathbf{0} \end{bmatrix} (\mathbf{u} + \mathbf{d}) \quad (22)$$

where the notation \mathbf{I} denotes the identity matrix.

4.2. LQIR-DG Control Scheme with Integral Action

In the proposed controller scheme, two fundamental players are selected in accordance with the game theory approach. The primary player determines the control commands, while another player generates the worst possible disturbance. To achieve the primary objective, first player minimizes the following cost function but the other player maximize it:

$$\min_u \max_d J(\mathbf{x}_{a_i}, d_i, u_i) = \min_d \max_u \int_0^{t_f} \left(\mathbf{x}_{a_i}^T \mathbf{Q}_i \mathbf{x}_{a_i} + u_i^T R u_i - d_i^T R_d d_i \right) dt \quad (23)$$

where t_f is the stop time and i -index denotes roll, pitch, ans yaw channels of the quadrotor. \mathbf{Q}_i , R_d , and R are weight coefficients of the cost function. By solving the above problem, the optimal control command is computed as follows [3]:

$$u_i = -\mathbf{K}_i \mathbf{x}_{a_i} \quad (24)$$

Moreover, the worst disturbance is obtained as

$$d_i = \mathbf{K}_{d_i} \mathbf{x}_{a_i} \quad (25)$$

Here, \mathbf{K}_{d_i} and \mathbf{K}_i are gain values defined as follows:

$$\mathbf{K}_{d_i} = R_d^{-1} \mathbf{B}_{a_{d_i}}^T \mathbf{P}_{a_{d_i}} \quad (26)$$

$$\mathbf{K}_i = R^{-1} \mathbf{B}_{a_i}^T \mathbf{P}_{a_i} \quad (27)$$

\mathbf{P}_{a_i} and $\mathbf{P}_{a_{d_i}}$ satisfy

$$-\mathbf{A}_a^T \mathbf{P}_{a_{d_i}} - \mathbf{Q}_i - \mathbf{P}_{a_{d_i}} \mathbf{A}_a + \mathbf{P}_{a_{d_i}} \mathbf{S}_{a_i} \mathbf{P}_{a_i} + \mathbf{P}_{a_{d_i}} \mathbf{S}_{a_{d_i}} \mathbf{P}_{a_{d_i}} = \mathbf{0} \quad (28)$$

$$-\mathbf{A}_a^T \mathbf{P}_{a_i} - \mathbf{Q}_i - \mathbf{P}_{a_i} \mathbf{A}_a + \mathbf{P}_{a_i} \mathbf{S}_{a_{d_i}} \mathbf{P}_{a_{d_i}} + \mathbf{P}_{a_i} \mathbf{S}_{a_i} \mathbf{P}_{a_i} = \mathbf{0} \quad (29)$$

where $\mathbf{S}_{a_i} = \mathbf{B}_{a_i} R^{-1} \mathbf{B}_{a_i}^T$ and $\mathbf{S}_{a_{d_i}} = \mathbf{B}_{a_{d_i}} R_d^{-1} \mathbf{B}_{a_{d_i}}^T$.

5. Results

The results of the parameter identification and the LQIR-DG Controller for the quadrotor platform are presented. First, the quadrotor parameters are estimated based on the NLS method. Oerformance of the LQIR-DG structure is evaluated. Moreover, Tables 1 and 2 presents the quadrotor and LQIR-DG parameters, respectively.

Table 1: Quadrotor parameters

Parameter	Unit	Value	Parameter	Unit	Value
d _{cg}	m	0.2	I _{xx}	kg.m ²	0.02839
d	N.m.sec ² /rad ²	3.2×10^{-6}	I _{yy}	kg.m ²	0.03066
b	N.sec ² /rad ²	3.13×10^{-5}	I _{zz}	kg.m ²	0.0439
Ω_{mean}	rpm	3000	I _{rotor}	kg.m ²	4.4398×10^{-5}

Table 2: LQIR-DG controller parameters

Channel	Weighting Matrix	Values
Roll	\mathbf{Q}_{roll}	diag([0.02, 65.96, 83.04, 0.00])
Pitch	$\mathbf{Q}_{\text{pitch}}$	diag([435.01, 262.60, 262.60, 0.00])
Yaw	\mathbf{Q}_{yaw}	diag([4×10^{-4} , 0.00, 0.133, 0])
-	R	1
-	R_d	1.2764

5.1. Identification of the 3DoF quadrotor platform model

As described in section 3.3, the parameters of the quadrotor platform, denoted by $\Gamma_i (i = 1, \dots, 8)$, are identified using the NLS-TRR algorithm. To increase accuracy of parameter identification, three scenarios are considered according to Table 3. In the first scenario, depicted in Figure 5, the quadrotor rotates about only one axis (roll, pitch, or yaw axes) to identify the parameters Γ_3 , Γ_6 , and Γ_8 . In the second scenario, according to Figure 6, the parameters Γ_2 and Γ_5 are estimated by rotating the experimental platform around its roll and pitch axes simultaneously. Finally, Figure 7 displays the results of the third scenario including the estimation of the parameters Γ_1 , Γ_4 , and Γ_7 for the UAV model when the platform freely rotates around three axes. After the termination condition is met, the optimal values of the quadrotor parameters are computed and denoted in Table 4. These results illustrate that the outputs of the simulation results for the quadrotor model are consistent with reality.

Table 3: Scenarios for identification of quadrotor parameters.

Scenario	Description	Initial Condition (deg)			Rotational Velocity Commands (rpm)			
		ϕ	θ	ψ	Ω_1	Ω_2	Ω_3	Ω_4
I	roll free	38	-	-	2000	2000	2000	3400
	pitch free	-	-15	-	3700	2000	2000	2000
	yaw free	-	-	-75	2000	3300	2000	3300
II	roll & pitch free	8	-5	-	1700	3800	2400	1700
III	roll, pitch, & yaw free	8	-3	-146	1700	3800	2400	1700

Table 4: True values of the quadrotor parameters.

Parameter	Value	Parameter	Value
Γ_1	-0.9622	Γ_5	3.6441×10^{-4}
Γ_2	-0.0154	Γ_6	7.5395×10^{-5}
Γ_3	5.4716×10^{-5}	Γ_7	0.1308
Γ_4	1.0457	Γ_8	4.3753×10^{-5}

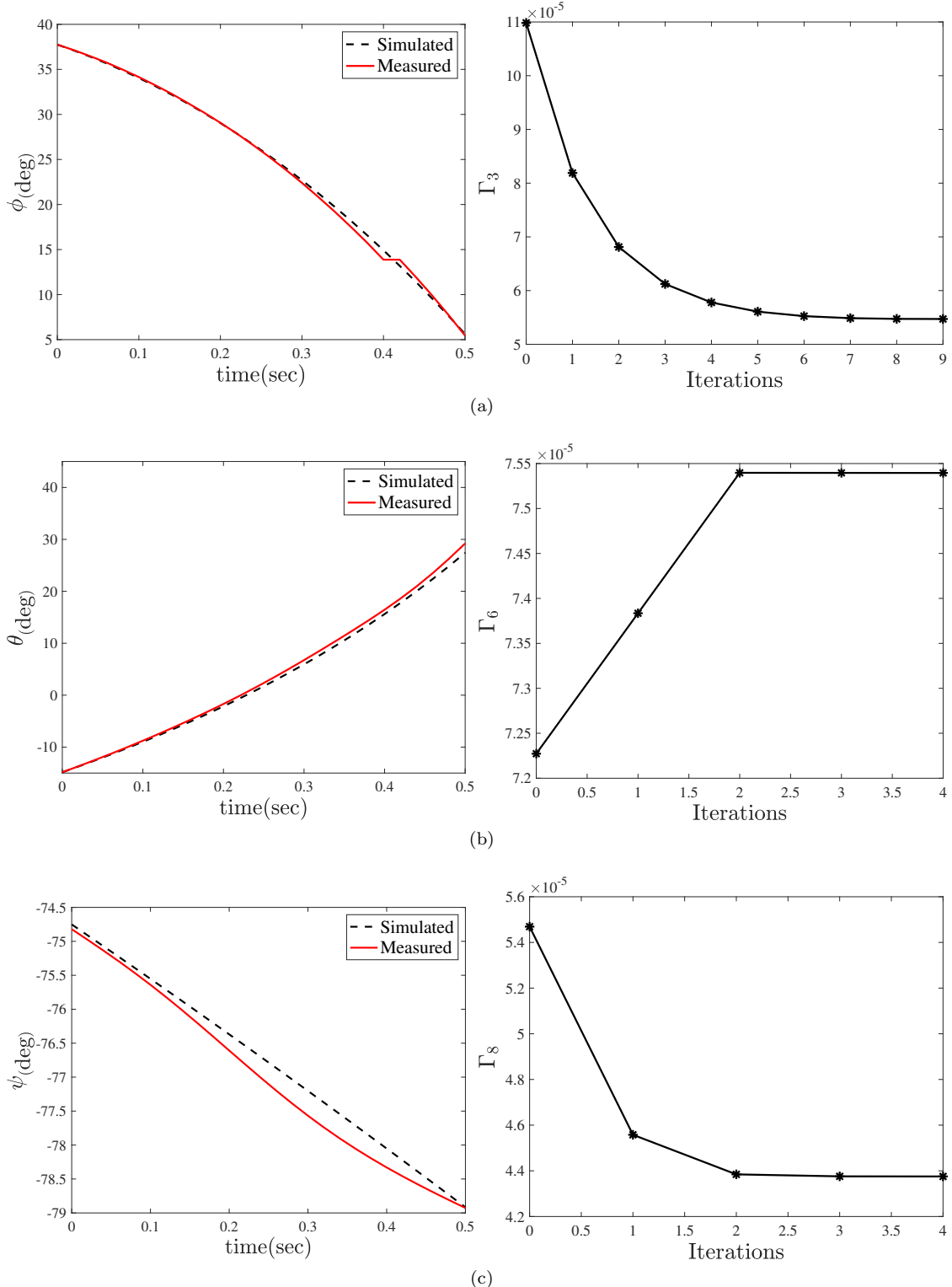


Figure 5: Identification process results when the quadrotor rotates about only one axis: (a) Identification of Γ_3 in free roll motion. (b) Identification of Γ_6 in free pitch motion. (c) Identification of Γ_8 in free yaw motion.

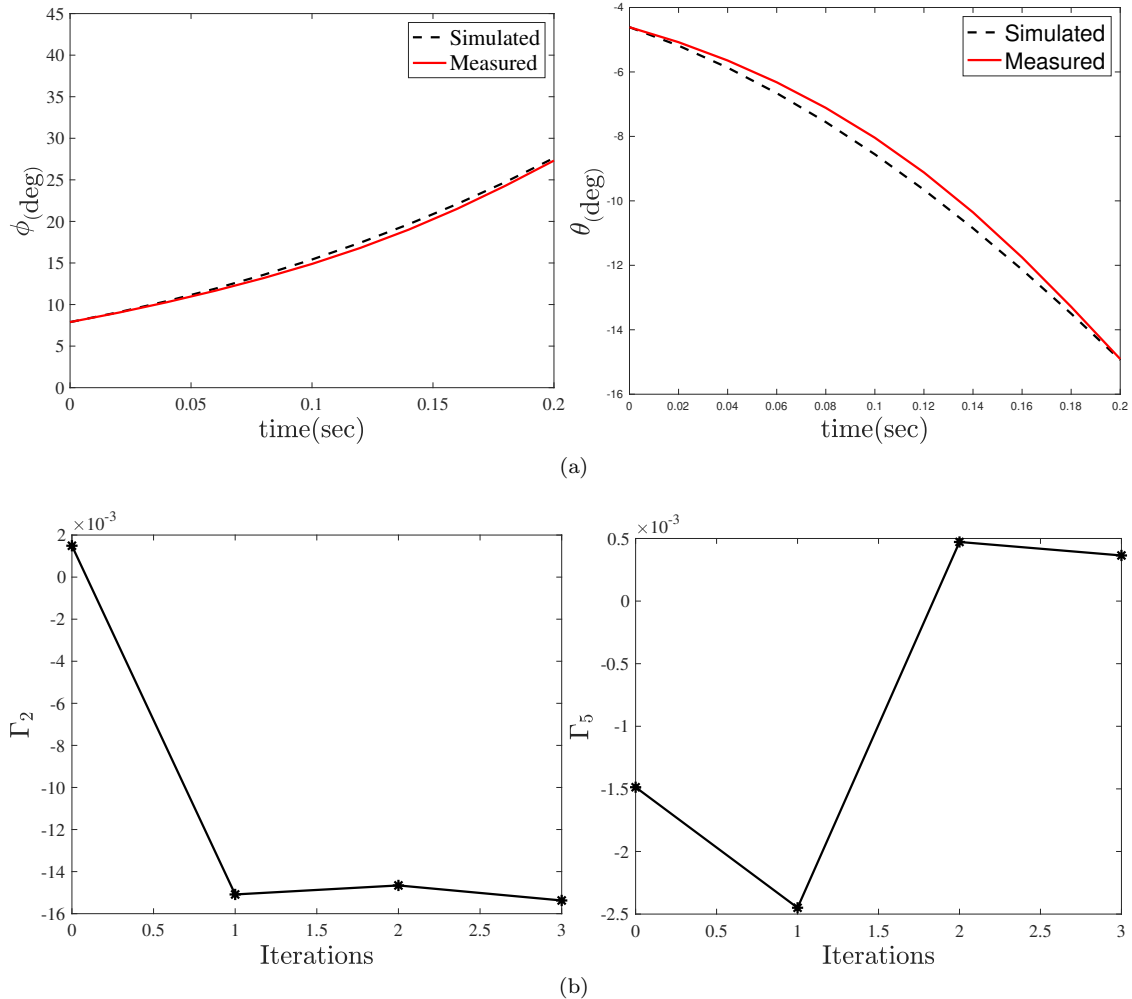


Figure 6: Identification process results when the quadrotor rotates about its roll and pitch axes: (a) Comparison of Simulation and experimental results. (b) Identification of Γ_2 and Γ_5 .

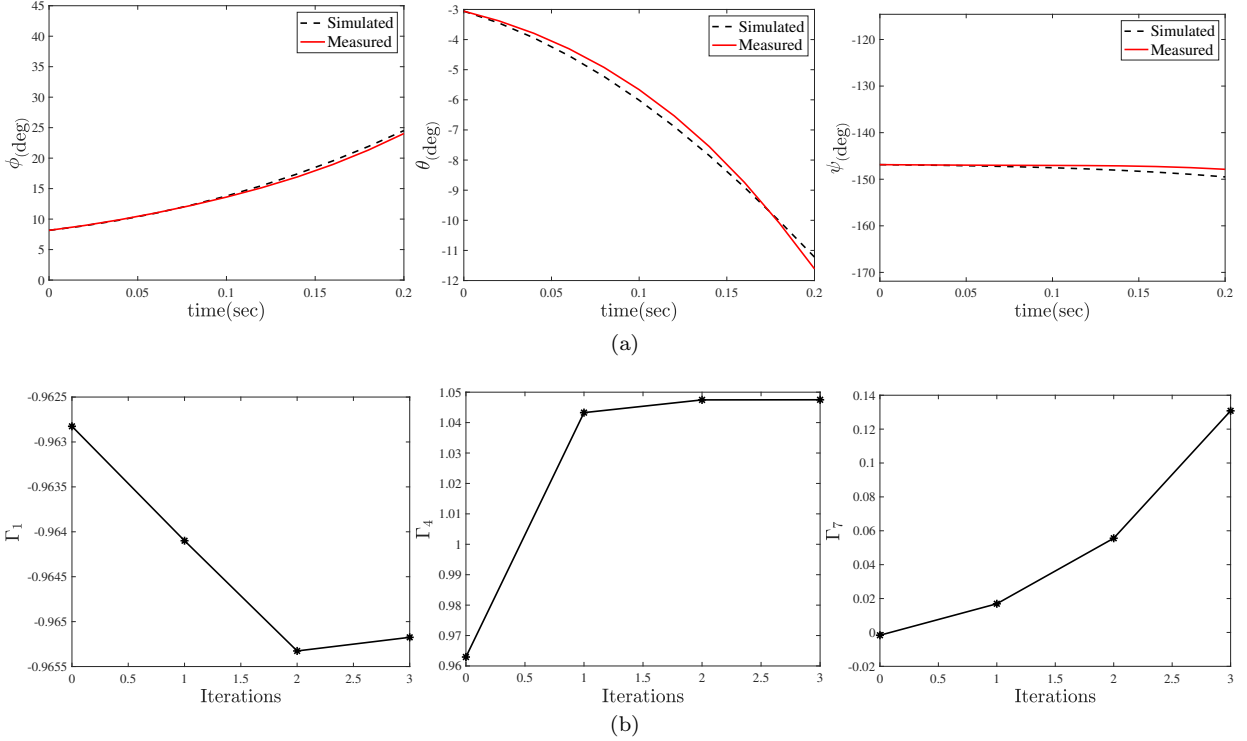


Figure 7: Identification process results when the quadrotor rotates about its roll, pitch, and yaw axes: (a) Comparison of Simulation and experimental results. (b) Identification of Γ_1 , Γ_4 and Γ_7 parameters.

5.2. Evaluation of LQIR-DG Performance

In this section, the LQIR-DG controller algorithm is evaluated in three scenarios i) regulation and tracking problems, ii) disturbance rejection, and iii) impact of model uncertainty. Finally, a comparison of the proposed controller is performed with a PID controller and variants of the LQR controller. The PID controller parameters are presented in Table 5.

Table 5: PID controller parameters

Channel	K_p	K_i	K_d
roll	18	6	9
pitch	22	15	16

5.2.1. Investigating of the Regulation and Tracking Problems

The results of the proposed approach are presented for tracking the desired roll and pitch angles of the experimental platform in Figures 8 and 9. Figure 8 (a) compares the desired and output signals, i.e., the euler angles during regulation problem. Moreover, Figure 8 (b) compares the desired square wave input with a frequency of 0.02 Hz and an amplitude of 20 degrees (with the output signals when the quadrotor platform freely rotates around roll and pitch simultaneity). Figures 9 (a) and (b) show the rotational velocity command of the quadrotor in the regulation and tracking problems, respectively. These results demonstrate that the roll and pitch angles are accurately controlled by the proposed approach.

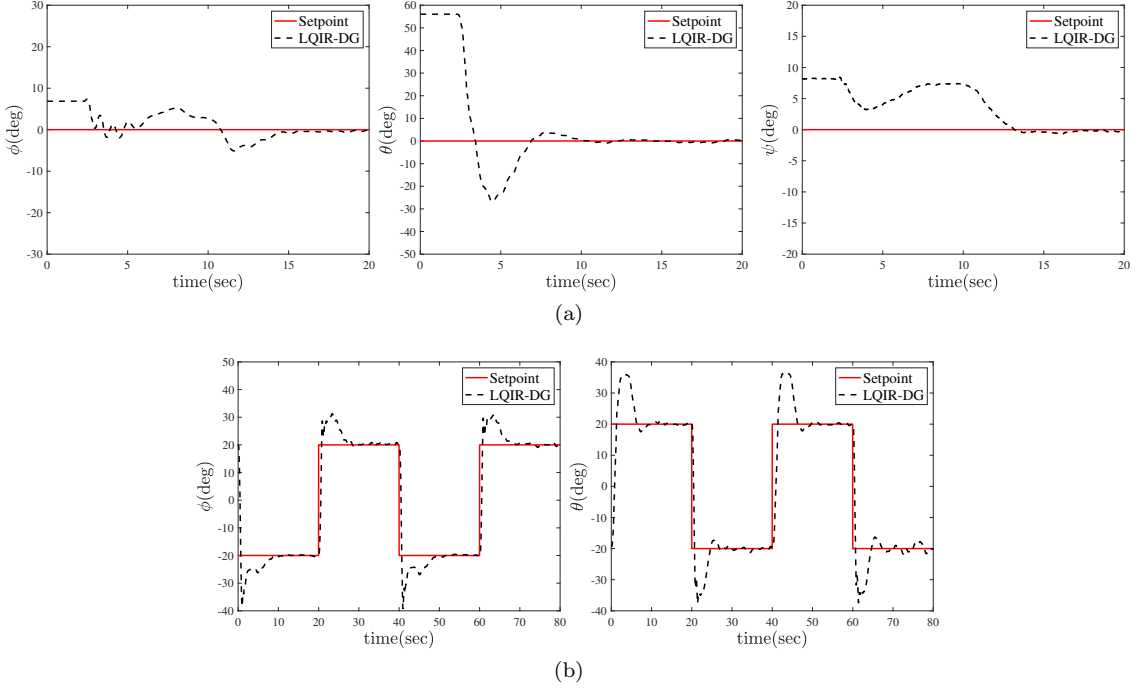


Figure 8: Comparison of actual roll and pitch angles with the desired values in (a) Regulation (b) Tracking problem.

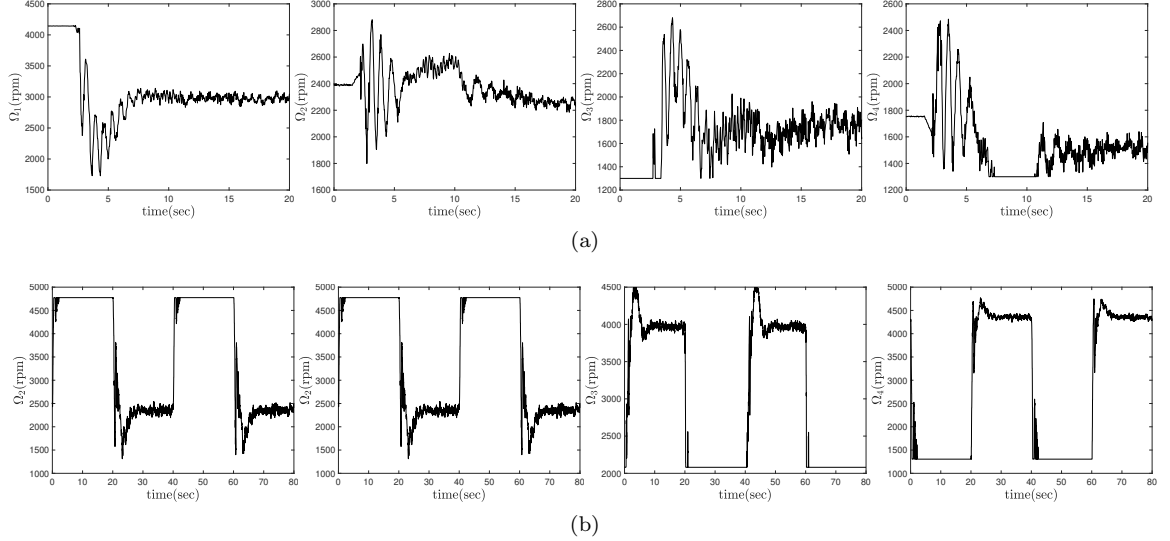


Figure 9: Rotational velocity commands in (a) Regulation (b) Tracking problems.

5.2.2. Investigating the Disturbance Rejection

Here, the effect of the input disturbance is investigated on the performance of the propose controller. The input disturbance, d_{Ω_i} , is considered as a change in the command of the rotational velocity, modeled as

$$d_{\Omega_1} = d_{\Omega_2} = -d_{\Omega_3} = -d_{\Omega_4} = \begin{cases} 500 \text{ rpm} & 20 < t < 60 \\ 0 & \text{other} \end{cases} \quad (30)$$

Figure 10 illustrates the roll and pitch angles in the regulation problem when the input disturbance occurs. These results indicate that the LQIR-DG controller can stabilize the quadrotor platform in the presence of input disturbance.

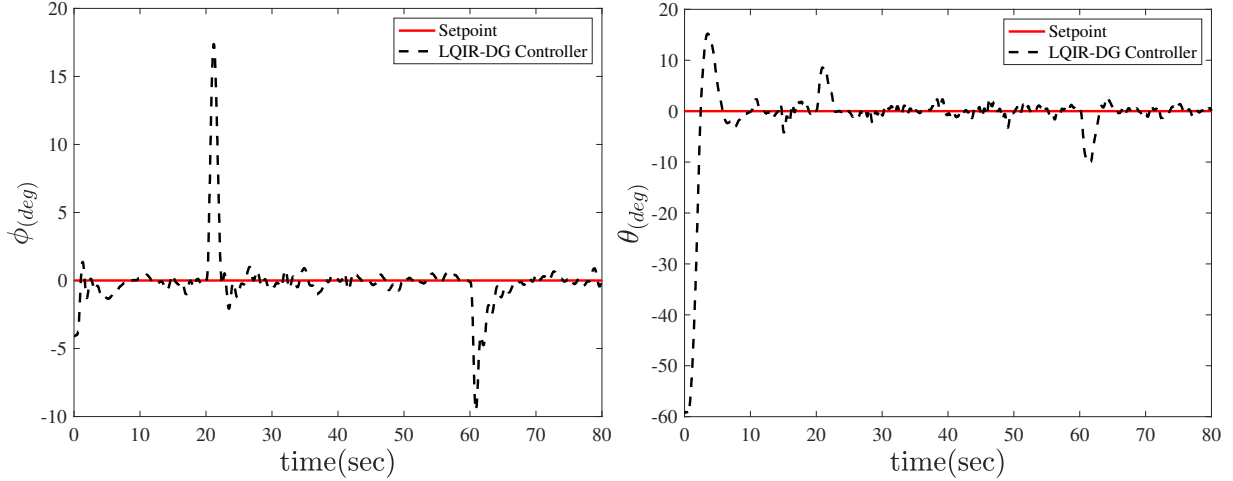


Figure 10: Comparison of actual roll and pitch angles with the desired, when the input disturbance occurs.

5.2.3. Investigating the Impact of Modeling Uncertainty

The effect of the modeling uncertainty is investigated on the performance of the propose controller. To achieve this, 50 and 100 grams weights are added to the roll and pitch axes, respectively, as shown in Figure 11. Figure 12 (a) compares the desired and the actual roll angle and Figure 12 (b) shows the desired and the actual pitch angle when the uncertainty of moments of inertia is present. Moreover, Figure 12 (c) shows the rotational velocity command of the experimental platform when the model uncertainty is applied. The implementation results show that the proposed controller converges to the desired values in the presence of the modeling uncertainty.

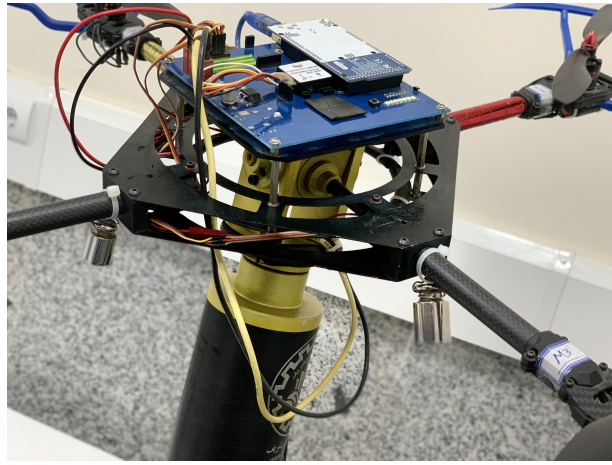


Figure 11: Quadrotor 3DoF platform with added weights.

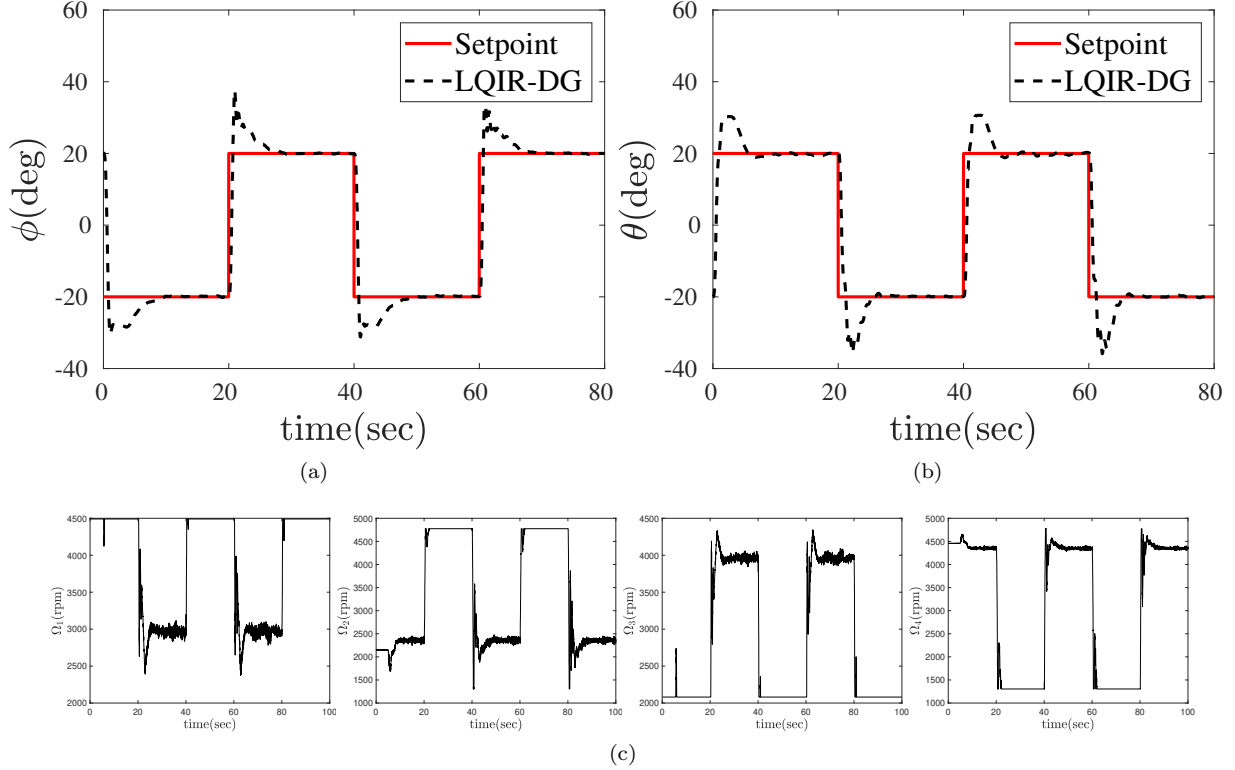


Figure 12: Comparison of actual roll and pitch angles with desired values, when the modeling uncertainty is present.

5.2.4. Comparison with the Control Strategies

Figure 13 compares the LQIR-DG controller performance with the PID controller and variant of the LQR strategies such as the LQR and LQIR. Moreover, the box plot of all controllers is plotted in Figure 14 for the cost function, introduced in equation (23). The median of RMSE is shown in the crossline in the box plot. These results indicate that the proposed controller is able to provide rapid convergence and excellent transient response relative to other controllers for attitude control of the experimental platform

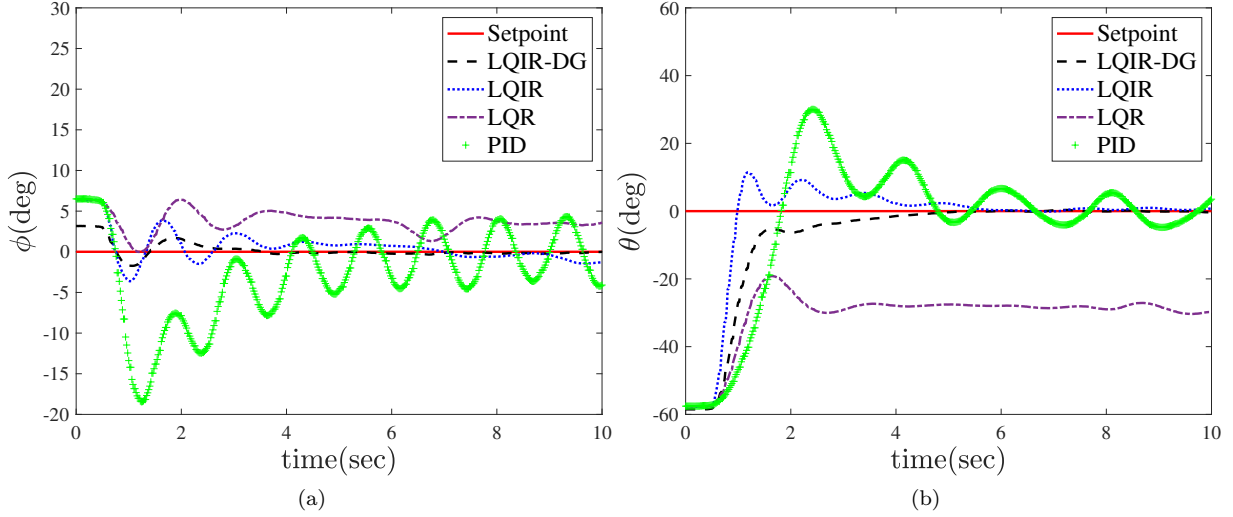


Figure 13: Comparison of LQIR-DG structure with the variant of LQR and PID in regulation problem: (a) Roll Angle (b) Pitch Angle.

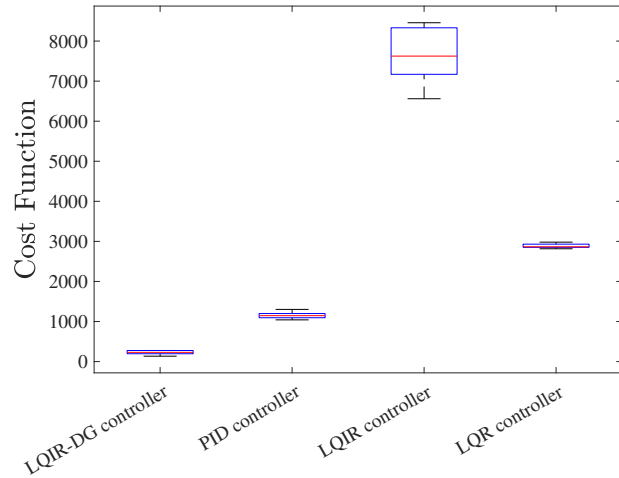


Figure 14: Box plot of LQIR-DG, LQR, LQIR, and PID controllers.

6. Conclusion

In this paper, the LQR controller with integral action based on the game theory called, LQIR-DG, was used in real-time for attitude control of platform quadrotor. For the implementation of the controller structure, an accurate dynamic model was considered for the experimental platform. Then, the model parameters were identified using the NSL method. For evaluation of the proposed method, the purposes where regulation and tracking problems were successfully performed. Moreover, the ability of the proposed method was investigated in rejection of the input disturbance and modeling error in the laboratory experiment. The implementation results illustrated the excellent performance of the LQIR controller based game theory approach in attitude control for the quadrotor platform.

References

- [1] Bouabdallah, S., 2007. Design and control of quadrotors with application to autonomous flying doi:10.5075/epfl-thesis-3727.

- [2] Bouabdallah, S., Siegwart, R., 2007. Full control of a quadrotor, in: 2007 IEEE/RSJ International Conference on Intelligent Robots and Systems, pp. 153–158. doi:10.1109/IROS.2007.4399042.
- [3] Engwerda, J., 2006. Linear Quadratic Games: An Overview. WorkingPaper. Macroeconomics. Subsequently published in Advances in Dynamic Games and their Applications (book), 2009 Pagination: 32.